Metastable rocksalt ZnO is *p*-type dopable

Anuj Goyal and Vladan Stevanović*
Colorado School of Mines, Golden, Colorado 80401, USA
and National Renewable Energy Laboratory, Golden, Colorado 80401, USA

(Received 20 February 2018; published 20 August 2018)

Despite decades of efforts, achieving *p*-type conductivity in the wide band gap ZnO in its ground-state wurtzite structure continues to be a challenge. Here we detail how *p*-type ZnO can be realized in a known metastable, high-pressure rocksalt phase (also wide-gap) with Li as an external dopant. Using modern defect theory, we predict Li to dope the rocksalt phase *p*-type by preferentially substituting for Zn and introducing shallow acceptor levels, resulting in predicted hole concentrations to exceed 10^{19} cm^{-3}. Formation of compensating donors like interstitial Li and unintentional hydrogen, ubiquitous in wurtzite phase, is inhibited by the close-packed nature of the rocksalt polymorph. Also, relatively high absolute valence band edge of rocksalt ZnO benefits low hole effective masses and hole delocalization. In addition to the technological significance, our results reveal polymorphism as a promising route to overcome strong doping asymmetry of wide band gap oxides.

DOI: 10.1103/PhysRevMaterials.2.084603

I. INTRODUCTION

Absence of a high-mobility *p*-type transparent semiconductor material represents a critical bottleneck for realizing active bipolar transparent electronics [1–5]. Strong proclivity of wide band gap semiconductors, oxides in particular, to *n*-type conductivity, limits current applications to unipolar and/or passive [4,5]. Following the work on GaN [6], significant efforts have been made in realizing *p*-type ZnO, however, only with limited success [7]. Despite its practical advantages over GaN, due to natural abundance and the more facile synthesis, ZnO in its ground state wurtzite structure strongly opposes *p*-type doping. This behavior of ZnO is well understood and follows mainly from the relatively low position of its band edges on the absolute energy scale that promotes both localization of holes (formation of deep acceptor states) and the pronounced donor behavior of ubiquitous impurities such as interstitial hydrogen [8,9]. The external *p*-type dopants, such as the group-V (N, P, As) substitutes for oxygen or group-I (Li, Na) substitutes for Zn, typically act as deep acceptors and/or are compensated by the donor defects such as oxygen vacancies or interstitial hydrogen [7–10]. Small atoms like Li or Na also self-compensate in the wurtzite structure by acting both as (deep) acceptors when substituting for Zn and shallow donors as interstitial impurities [8,11–13].

Here, we investigate whether polymorphism could be helpful in achieving *p*-type doping in ZnO. There are several reasons that make changing the crystal structure a plausible route to overcome doping bottlenecks of ZnO. First, changing the volume and local coordination could impact the formation of compensating donor defects. In particular, the high-pressure denser phases offer less interstitial space, which raises the energy to form interstitial defects, in particular interstitial hydrogen or group-I elements. Second and as important, higher energy polymorphs can be expected to have their valence band edge closer to vacuum, which is beneficial for the *p*-type doping [14] and for the formation of shallow acceptor levels. The expectation of valence band edge closer to vacuum follows from higher total energy of the metastable polymorph, because the total energy includes summation over all occupied electronic states [15].

In addition to the ground state wurtzite, ZnO is known to exist in the metastable zincblende and rocksalt structures [7]. The high-pressure rocksalt phase forms at about ∼9 GPa and can be stabilized at ambient conditions in the nanocrystalline form [16–18] or as thin film grown on the MgO substrate with about 15% of MgO alloyed [19,20]. This phase of ZnO is specifically relevant for our discussion because of its octahedral coordination of atoms, smaller volume (about 18% reduction) relative to the ground state wurtzite structure and predicted higher valence band edge (∼1 eV closer to vacuum) than the wurtzite [21]. Furthermore, previous demonstration of activated *p*-type transport in Li doped rocksalt MgO [22] supports the prospects of the rocksalt structure for alleviating self-compensation of Li impurities.

II. COMPUTATIONAL APPROACH

We use modern first-principles defect calculations based on hybrid density functional theory [23], to study intrinsic defect chemistry, the role of Li as a *p*-type dopant as well as the compensation by unintentional hydrogen in both ground state wurtzite and the metastable rocksalt phase. We employ a standard supercell approach to calculate formation energy $\Delta H_{D,q}$ of a point defect D in the charge state q using the following equation:

$$\Delta H_{D,q}(E_F, \mu) = [E_{D,q} - E_H] + \sum_i n_i \mu_i + q E_F + E_{corr}, \quad (1)$$

*vstevano@mines.edu

where, $E_{D,q}$ and E_H are the total energies of the supercells with and without the defect, respectively, $\{\mu_i\}$ are the chemical potentials of different atomic species describing exchange with respective reservoirs, E_F is the Fermi energy, and E_{corr} is the finite-size correction term [23]. The chemical potential $\mu_i = \mu_i^0 + \Delta\mu_i$ is expressed relative to the reference elemental chemical potential μ_i^0, calculated using the FERE approach [24] (re-fitted for HSE calculations, see Supplemental Material [25]), and $\Delta\mu_i$ the deviation from the reference elemental phase, bounds of which are determined by the thermodynamic phase stability. The fraction of exchange mixing in the hybrid HSE functional [26,27] is adjusted for each structure separately to match their experimental lattice constants and band gaps. Having defect formation energy allows thermodynamic modeling of defect and carrier concentrations, computed here using the approach from Ref. [28]. Confidence in our predictions stems from the correct description of defects and doping in the wurtzite ZnO as well as from our previous works [29,30], demonstrating good agreement between calculated and measured defect and charge carrier concentrations in other systems.

All calculations are performed using the VASP code [31], hybrid exchange-correlation functional HSE06 [26,27] and the exchange mixing of $\alpha = 0.3$ for rocksalt and $\alpha = 0.375$ for wurtzite ZnO to match their experimental lattice parameters and their band gaps. The DFT portion of the hybrid HSE functional used the generalized gradient approximation of Perdew Burke Ernzerhof (PBE) [32]. Electronic cores are described within the projector augmented wave (PAW) method [33] as implemented in the VASP code. A 64 atom supercell and a Γ-centered $2 \times 2 \times 2$ k-point mesh [34] is used for defect calculations of the rocksalt ZnO. Convergence of the results is validated using a 216 atom supercell. In the wurtzite ZnO defect calculations are performed on a 96 atom supercell with a single Γ point. Calculations of defect formation energies, charge transition levels, and band edge energies relative to the vacuum level are performed using the standard approach described in Refs. [30,35]. Details of convergence tests and additional results with HSE and DFT-PBE are summarized in the Supplemental Material [25].

III. RESULTS AND DISCUSSION

As illustrated in Fig. 1, our results reproduce well the known behavior of Li impurities in the wurtzite structure which simultaneously act as substitutional acceptors and interstitial donors. From the predicted defect concentrations, shown in the left bottom panel of Fig. 1, it is evident that the self-compensation of Li is nearly complete, leading to very low net hole concentrations in the 10^{15}–10^{16} cm^{-3} range at temperatures well above 1000 K under O-rich synthesis conditions. These results are consistent with available experimental evidence and previous calculations of Li doping in wurtzite ZnO [10,36].

However, in the rocksalt structure, we predict a marked difference in the concentration of substitutional and interstitial Li, resulting in the net concentration of free holes to exceed 10^{19} cm^{-3} under the same synthesis conditions. The charge carrier (hole) concentrations of this magnitude make the Li-doped rocksalt ZnO a serious contender for the p-type transparent conductor applications [3–5]. As depicted in Fig. 1, calculated concentration of free holes closely follows that of

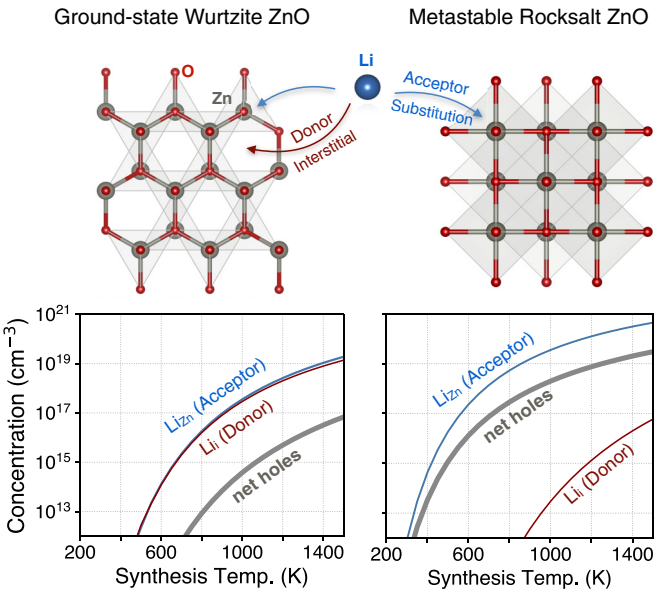

FIG. 1. Ground state wurtzite and metastable rocksalt ZnO structures are shown (upper panel) together with lattice sites Li impurities occupy. In the rocksalt phase Li preferentially substitutes for Zn and acts as a shallow acceptor leading to orders of magnitude higher hole concentrations (lower panel) shown for both structures at O-rich conditions and as a function of synthesis temperature.

substitutional Li_{Zn}, while the interstitial Li_i is predicted to be more than two orders of magnitude less abundant. The difference between the amount of Li_{Zn} and the number of free holes is due to the presence of compensating oxygen vacancies which become more favorable when Fermi energy approaches the valence band.

Figure 2 (upper panel) presents the standard defect formation energy plots that form the basis for predicting defect and charge carrier concentrations. Lines with positive slopes represent donor defects, negative slopes are the acceptors, and horizontal lines represent the charge-neutral defects. Energy at which a given defect changes its charge state are typically referred to as the thermodynamic charge transition levels. Dashed lines represent the equilibrium position of the Fermi energy established by the charge neutrality condition between charged defects and free charge carriers. For clarity we show in Fig. 2 only the lowest energy acceptor defect Li_{Zn} and the most relevant, potentially compensating, donors including Li_i, O vacancies (V_O), Zn interstitials (Zn_i), and H interstitials (H_i). A complete picture that comprises all point defects and defect complexes is provided in the Supplemental Material [25].

Defect formation energy plots in Fig. 2 clearly show the compensation between Li_{Zn} and Li_i in the wurtzite structure. In addition, the compensating interstitial (unintentional) hydrogen is only 0.26 eV higher in formation energy than Li_i. Other donors such as V_O and Zn_i are less relevant due to their higher formation energy. Calculated equilibrium Fermi energy is about 1.2 eV above the valence band edge and is only weakly temperature dependent. Hence, the achievable hole concentrations in wurtzite ZnO are very low and are predicted to not exceed 10^{17} cm^{-3} even at very high synthesis temperatures. Also, the defect states created by Li_{Zn} are localized,

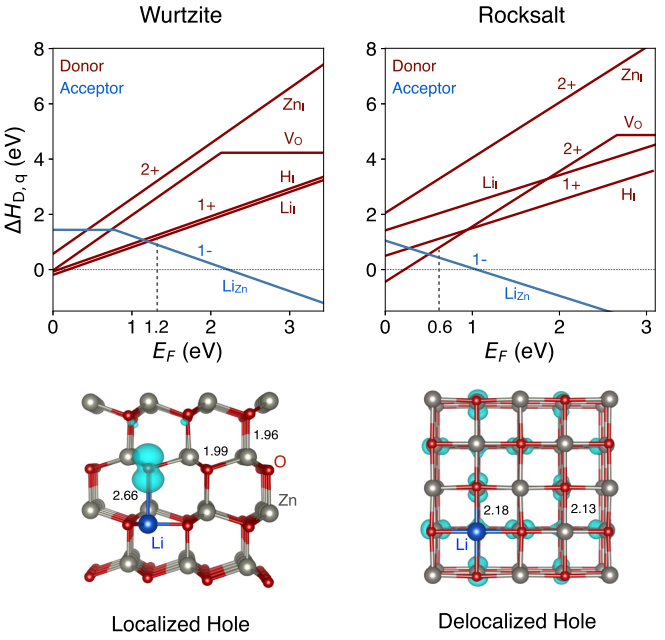

FIG. 2. Calculated defect formation energies at O-rich conditions as a function of the Fermi energy for both wurtzite and rocksalt ZnO (upper panel). Only the lowest energy Li_{Zn} acceptor defect is shown (blue) together with relevant competing donors Li_i, O-vacancy, Zn_i, H_i (red). Dashed lines mark the position of the equilibrium Fermi energy. (lower panel) Wave functions of the acceptor states are shown for Li^0_{Zn} defect in wurtzite and rocksalt ZnO.

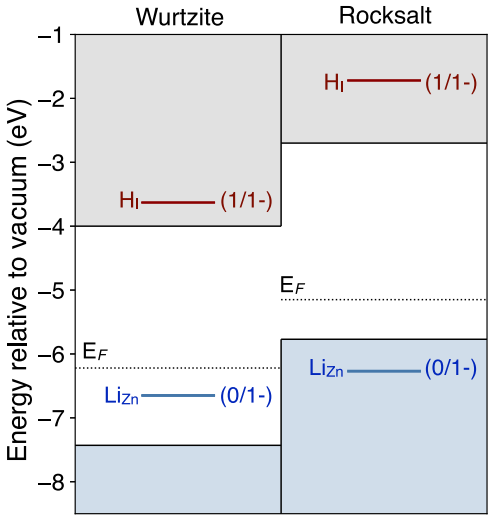

FIG. 3. Comparison of the calculated absolute band-edge energies of the wurtzite and rocksalt phases of ZnO. Charge transition states of substitutional Li and interstitial hydrogen are shown along with the position of the equilibrium Fermi energy (dashed lines) in both structures.

i.e., the small polarons with relatively high ionization energy (∼0.78 eV) are predicted to form, which restrict mobility of holes and overall conductivity in already weakly p-type wurtzite ZnO. This behavior is known [12,13,37] and well reproduced in our calculations. The localized, polaronic hole state in the wurtzite structure is shown in the lower panel of Fig. 2, where localization of a hole at one of the O atoms neighboring to the Li_{Zn} is evident.

The response of the rocksalt ZnO to Li impurities is markedly different. The formation of Li_{Zn} is clearly more favorable, while both Li_i and H_i are higher in formation energy. Furthermore, the holes created by the substitutional Li are delocalized and formation of small polarons is not favored by the rocksalt structure as shown in Fig. 2. We do however, find the localized hole state in the rocksalt structure (with localization on the neighboring oxygen), but this state is about 0.8 eV higher in energy than the delocalized valence band derived states (see Supplemental Material [25]). In the rocksalt structure the role of partially compensating donor is taken by V_O, which allows the equilibrium Fermi energy to approach much closer to the valence band. The Fermi energy is about 0.6 eV above the VBM, also weakly dependent on temperature, resulting in hole concentrations in excess of 10^{19} cm^{-3} at synthesis temperatures above 1200 K. From the effective mass theory [12,13], we estimate the ionization energy of holes in rocksalt ZnO to be ∼6 meV, which is practically negligible for the purpose of our discussion. The shallow nature of Li_{Zn} acceptor implies nearly 100% doping efficiency (one hole per every Li_{Zn} acceptor), and therefore, once can expect that in samples synthesized at high temperature and then quenched, the carrier concentration will closely follow the (frozen) high-temperature values. Formation of defect complexes such as $Li_{Zn} + V_O$, $2Li_{Zn} + V_O$ or $Li_{Zn} + Li_i$ does not alter the results as shown in the Supplemental Material [25].

Another very important feature of the rocksalt ZnO is its bipolar doping nature. Namely, in the absence of Li and at O-poor conditions rocksalt ZnO remains n-type dopable. Our investigation of the intrinsic defects clearly indicates that at O-poor conditions the absence of low-energy acceptors allows extrinsic n-type doping (defects plots provided in the Supplemental Material [25]). While the predicted intrinsic electron concentrations of ∼10^{18} cm^{-3} are relatively low, there is no reason to believe that higher electron concentrations could not be attained using external dopants.

A. Why is rocksalt ZnO p-type dopable?

Per previous discussion, the increase in the formation energy of interstitial compensating donors, such as Li_i and H_i, can be attributed in part to the higher density of the rocksalt structure which leaves less interstitial space. However, higher formation energies of *charged* donors can also be due to the higher absolute position of the band edges. Indeed, as shown in Fig. 3 both band edges of the rocksalt phase are closer to vacuum than those of the wurtzite phase, VBM is calculated to be by approximately 1.6 eV higher and CBM is by 1.3 eV. Nevertheless, the effects of the smaller volume can be seen by examining the interstitial hydrogen. If only the band edge position were to contribute, then the absolute position of the $1+/1-$ hydrogen charge transition level should remain unchanged between the two structures. Figures 2 and 3 clearly show that this is not the case and that the H_i charge transition level is closer to vacuum in the rocksalt structure. This behavior can be explained by the higher density of the rocksalt structure, which due to less interstitial space affects the formation energy of H_i more in the $1-$ charge state

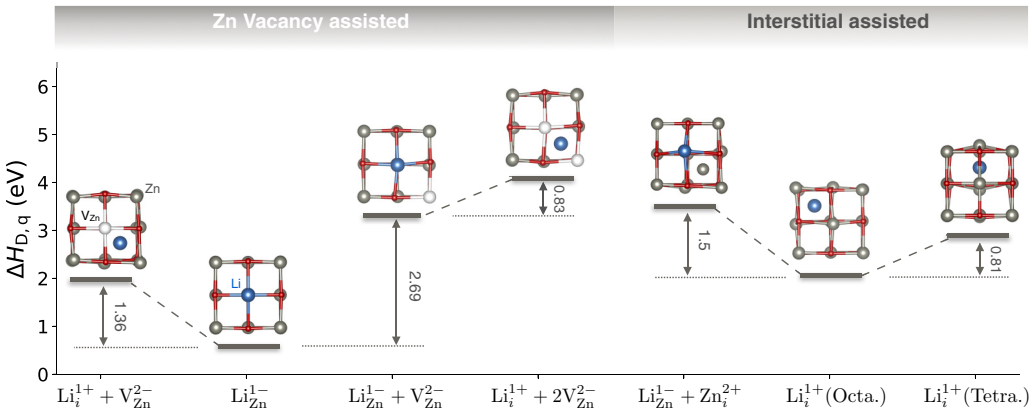

FIG. 4. Formation energies of various defects and defect complexes associated with Li-ion migration in the rocksalt ZnO are shown at the equilibrium Fermi energy under O-rich growth conditions. Mechanisms are broadly classified into (a) Zn vacancy assisted and (b) interstitial (either Zn or Li) assisted.

(H^- ion) than in the 1+ charge state (bare proton). As a result, the H(1 + /1−) charge transition level in the denser phase is closer to vacuum. It is important to note that this behavior does not follow the universal alignment of H(1 + /1−) level in semiconductors of Van de Walle and Neugebauer [38]. Similar deviations from this universal behavior have also been shown in semiconductors such as diamond and cubic-BN indicating the important role the volume plays for interstitial defects [39]. Furthermore, relatively good alignment of the $Li_{Zn}(0/1-)$ charge transition levels between the two structures is consistent with the expectation that the volume change affects more interstitial than the substitutional defects. Therefore, the misalignment of the H(1 + /1−) levels might suggest the existence of different universality classes that correspond to different crystal structures and/or local coordination.

B. Prospects for application of rocksalt ZnO

As already noted the *p*-type dopability of rocksalt ZnO as well as its bipolar nature could be transformative in the context of *p*-type transparent conducting oxides and transparent electronics in general. In addition to dopability, charge carrier mobility and optical transparency are relevant. Concerning the carrier mobility in the rocksalt ZnO, our results do not show reasons for concern. From the band structure calculations, we find VBM to be at the L point in the Brillouin zone (see Supplemental Material [25]) with the relatively low hole band effective mass $m_h \sim 0.4$ (units of the free electron mass), corresponding to the lighter of the two bands that are degenerate at the VBM. The conduction band is more dispersive with the electron band effective mass $m_e \lesssim 0.2$. Concerning the ionized impurity scattering in the Li-doped rocksalt ZnO, the shallow nature of Li_{Zn} with the localized polaronic state appearing as a resonance deep in the valence band could be considered less detrimental to transport than the deep defects with states in the band gap [40]. In regard to the optical transparency, we calculate the band gap of rocksalt ZnO to be indirect and close to 3.1 eV, in good agreement with many-body GW calculations of S. Lany [21]. Hence, all direct interband transitions lay above the visible part of the solar spectrum. Also, from the band structure we find that only weak intraband transitions are possible for both holes and electrons as most of the direct transitions from the band edges into the bands either require energies larger than 3 eV or are between O-2p derived states (holes) and are likely to have low oscillator strengths. Additionally, predicted hole concentrations and effective masses imply the plasma frequency in the far infrared, which removes concerns related to the plasmon excitations.

C. Possible synthesis routes and stability of Li-doped rocksalt ZnO

While the rocksalt phase of ZnO has been stabilized at ambient condition [16–19], doping with Li has not been attempted before. Based on our results, *p*-type doping with Li is achievable at high temperatures under O-rich conditions that can be maintained by employing highly reactive oxygen sources such as plasma or purified ozone in vacuum deposition techniques [41]. Note that the influence of MgO alloying, needed to stabilize rocksalt ZnO in thin film form, on Li doping and hole localization requires additional investigation. However, once O-rich thin films are achieved, Li diffusion in the rocksalt ZnO can be of concern in relation to the stability of the *p*-type material. In Fig. 4 we provide defect formation energies of different point defects and defect complexes that act as intermediate local minima along various Li diffusion pathways. Similar to the wurtzite structure in which Li diffusion has been previously studied [36], the energy differences between different local minima are relatively high. Diffusion of substitutional Li via interstitial sites (leaving behind the Zn vacancy) requires overcoming at least the energy difference of 1.36 eV. The exchange of sites between Li_{Zn} and the neighboring V_{Zn} requires overcoming at least 0.83 eV but also requires the formation of a $Li_{Zn} + V_{Zn}$ complex which is high in energy. Direct diffusion of interstitial Li would require a minimum of 0.81 eV, but Li_i are higher in energy and much less abundant than the substitutional Li. Therefore, based on

our calculations facile diffusion of Li in the rocksalt ZnO is improbable.

IV. CONCLUSION

Using modern defect theory we have shown here that the p-type doping in ZnO could be achieved in the metastable, high-pressure rocksalt phase with Li as extrinsic dopant. Our predictions show that in the rocksalt phase extrinsic Li preferentially substitutes for Zn, creates shallow acceptor levels, and allows hole concentrations in excess of 10^{19} cm^{-3} at O-rich growth conditions. The combination of the close-packed structure and the high absolute band edge energies renders compensating donors such as interstitial Li and/or unintentional H, which are detrimental to p-type doping in the ground state wurtzite structure, high in formation energy, and are also responsible for the relatively low hole effective mass $m_h \sim 0.4$. Furthermore, we find that at O-poor conditions, rocksalt ZnO remains n-type dopable making this material even more interesting because of its bipolarity. We do understand that the utilization of metastable (high-pressure) phases in commercial applications might be challenging. However, there are examples of highly metastable materials, such as fullerenes (about 0.3 eV/atom higher in energy than ground state graphite [42]), that are presently being used in commercial applications [43]. Therefore, we are optimistic that with the current state-of-the-art high-pressure [44] and thin-film synthesis techniques [45], p-type doped metastable rocksalt ZnO is achievable. In our view, the return on investment should be worth an effort given the significance of transparent p-type rocksalt ZnO and its bipolar nature to transparent electronics in general.

ACKNOWLEDGMENTS

The authors thank Dr. Stephan Lany from National Renewable Energy Laboratory (NREL) for fruitful discussions. The work was supported as part of the Center for the Next Generation of Materials by Design, an Energy Frontier Research Center (EFRC) funded by U.S. Department of Energy (DOE), Office of Science, Basic Energy Sciences. This research used computational resources sponsored by the DOE Office of Energy Efficiency and Renewable Energy and located at NREL.

[1] G. Thomas, Nature (London) **389**, 907 (1997).
[2] H. Kawazoe, M. Yasukawa, H. Hyodo, M. Kurita, H. Yanagi, and H. Hosono, Nature (London) **389**, 939 (1997).
[3] J. F. Wager, Science **300**, 1245 (2003).
[4] J. F. Wager, D. A. Keszler, and R. E. Presley, *Transparent Electronics* (Springer US, Boston, MA, 2008).
[5] H. Hosono, D. C. Paine, and D. Ginley, *Handbook of Transparent Conductors*, edited by D. S. Ginley (Springer US, Boston, MA, 2011).
[6] S. Nakamura, Rev. Mod. Phys. **87**, 1139 (2015).
[7] Ü. Özgür, Y. I. Alivov, C. Liu, A. Teke, M. A. Reshchikov, S. Dogan, V. Avrutin, S.-J. Cho, and H. Morkoç, J. Appl. Phys. **98**, 041301 (2005).
[8] A. Janotti and C. G. Van de Walle, Rep. Prog. Phys. **72**, 126501 (2009).
[9] C. G. Van de Walle, Phys. Rev. Lett. **85**, 1012 (2000).
[10] M. D. McCluskey, C. D. Corolewski, J. Lv, M. C. Tarun, S. T. Teklemichael, E. D. Walter, M. G. Norton, K. W. Harrison, and S. Ha, J. Appl. Phys. **117**, 112802 (2015).
[11] C. H. Park, S. B. Zhang, and S.-H. Wei, Phys. Rev. B **66**, 073202 (2002).
[12] S. Lany and A. Zunger, Appl. Phys. Lett. **96**, 142114 (2010).
[13] J. L. Lyons, A. Janotti, and C. G. Van de Walle, J. Appl. Phys. **115**, 012014 (2014).
[14] S. B. Zhang, S.-H. Wei, and A. Zunger, J. Appl. Phys. **83**, 3192 (1998).
[15] J. Ihm, A. Zunger, and M. L. Cohen, J. Phys. C: Solid State Phys. **12**, 4409 (1979).
[16] F. Decremps, J. Pellicer-Porres, F. Datchi, J. P. Itié, A. Polian, F. Baudelet, and J. Z. Jiang, Appl. Phys. Lett. **81**, 4820 (2002).
[17] P. S. Sokolov, A. N. Baranov, Z. V. Dobrokhotov, and V. L. Solozhenko, Russ. Chem. Bull. **59**, 325 (2010).
[18] H. Razavi-Khosroshahi, K. Edalati, J. Wu, Y. Nakashima, M. Arita, Y. Ikoma, M. Sadakiyo, Y. Inagaki, A. Staykov, M. Yamauchi, Z. Horita, and M. Fuji, J. Mater. Chem. A **5**, 20298 (2017).
[19] M. Kunisu, I. Tanaka, T. Yamamoto, T. Suga, and T. Mizoguchi, J. Phys.: Condens. Matter **16**, 3801 (2004).
[20] C.-Y. J. Lu, Y.-T. Tu, T. Yan, A. Trampert, L. Chang, and K. H. Ploog, J. Chem. Phys. **144**, 214704 (2016).
[21] S. Lany, Proc. SPIE **8987**, 89870K (2014).
[22] M. M. Tardío, R. Ramírez, R. González, and Y. Chen, Phys. Rev. B **66**, 134202 (2002).
[23] C. Freysoldt, B. Grabowski, T. Hickel, J. Neugebauer, G. Kresse, A. Janotti, and C. G. Van de Walle, Rev. Mod. Phys. **86**, 253 (2014).
[24] V. Stevanović, S. Lany, X. Zhang, and A. Zunger, Phys. Rev. B **85**, 115104 (2012).
[25] See Supplemental Material at http://link.aps.org/supplemental/10.1103/PhysRevMaterials.2.084603 for comparison of the bulk properties and detailed defect diagrams at different levels of theory between rocksalt and wurtzite ZnO.
[26] J. Heyd, G. E. Scuseria, and M. Ernzerhof, J. Chem. Phys. **118**, 8207 (2003).
[27] J. Heyd, G. E. Scuseria, and M. Ernzerhof, J. Chem. Phys. **124**, 219906 (2006).
[28] K. Biswas and S. Lany, Phys. Rev. B **80**, 115206 (2009).
[29] A. Goyal, P. Gorai, H. Peng, S. Lany, and V. Stevanović, Comput. Mater. Sci. **130**, 1 (2017).
[30] A. Goyal, P. Gorai, E. S. Toberer, and V. Stevanović, npj Comput. Mater. **3**, 42 (2017).
[31] G. Kresse and J. Furthmüller, Comput. Mater. Sci. **6**, 15 (1996).
[32] J. P. Perdew, K. Burke, and M. Ernzerhof, Phys. Rev. Lett. **77**, 3865 (1996).

[33] P. E. Blöchl, Phys. Rev. B **50**, 17953 (1994).
[34] H. J. Monkhorst and J. D. Pack, Phys. Rev. B **13**, 5188 (1976).
[35] V. Stevanović, S. Lany, D. S. Ginley, W. Tumas, and A. Zunger, Phys. Chem. Chem. Phys. **16**, 3706 (2014).
[36] A. Carvalho, A. Alkauskas, A. Pasquarello, A. K. Tagantsev, and N. Setter, Phys. Rev. B **80**, 195205 (2009).
[37] S. Lany and A. Zunger, Phys. Rev. B **80**, 085202 (2009).
[38] C. G. Van de Walle and J. Neugebauer, Nature (London) **423**, 626 (2003).
[39] J. L. Lyons and C. G. Van de Walle, J. Phys.: Condens. Matter **28**, 06LT01 (2016).
[40] R. E. Brandt, V. Stevanović, D. S. Ginley, and T. Buonassisi, MRS Commun. **5**, 265 (2015).
[41] D. G. Schlom, APL Materials **3**, 062403 (2015).
[42] J.-T. Wang, C. Chen, E. Wang, and Y. Kawazoe, Sci. Rep. **4**, 4339 (2015).
[43] D. Jariwala, V. K. Sangwan, L. J. Lauhon, T. J. Marks, and M. C. Hersam, Chem. Soc. Rev. **42**, 2824 (2013).
[44] H.-K. Mao, X.-J. Chen, Y. Ding, B. Li, and L. Wang, Rev. Mod. Phys. **90**, 015007 (2018).
[45] A. Zakutayev, N. H. Perry, T. O. Mason, D. S. Ginley, and S. Lany, Appl. Phys. Lett. **103**, 232106 (2013).